Biosensors and Bioelectronics 67 (2015) 687–693

Contents lists available at ScienceDirect

Biosensors and Bioelectronics

journal homepage: www.elsevier.com/locate/bios

A reusable robust radio frequency biosensor using microwave resonator by integrated passive device technology for quantitative detection of glucose level

N.Y. Kim *, R. Dhakal, K.K. Adhikari, E.S. Kim, C. Wang

Department of Electronics Engineering, Kwangwoon University, Seoul, Republic of Korea

ARTICLE INFO

Article history:
Received 6 June 2014
Received in revised form
6 October 2014
Accepted 9 October 2014
Available online 19 October 2014

Keywords:
Glucose sensor
RF biosensor
Reusable biosensor
Microwave sensing
Real-time identification
Integrated passive device

ABSTRACT

A reusable robust radio frequency (RF) biosensor with a rectangular meandered line (RML) resonator on a gallium arsenide substrate by integrated passive device (IPD) technology was designed, fabricated and tested to enable the real-time identification of the glucose level in human serum. The air-bridge structure fabricated by an IPD technology was applied to the RML resonator to improve its sensitivity by increasing the magnitude of the return loss (S_{21}). The resonance behaviour, based on S_{21} characteristics of the biosensor, was analysed at 9.20 GHz with human serum containing different glucose concentration ranging from 148–268 mg dl^{-1}, 105–225 mg dl^{-1} and at a deionised (D) water glucose concentration in the range of 25– 500 mg dl^{-1} for seven different samples. A calibration analysis was performed for the human serum from two different subjects and for D-glucose at a response time of 60 s; the reproducibility, the minimum shift in resonance frequency and the long-term stability of the signal were investigated. The feature characteristics based on the resonance concept after the use of serum as an analyte are modelled as an inductor, capacitor and resistor. The findings support the development of resonance-based sensing with an excellent sensitivity of 1.08 MHz per 1 mg dl^{-1}, a detection limit of 8.01 mg dl^{-1}, and a limit of quantisation of 24.30 mg dl^{-1}.

1. Introduction

Diabetes mellitus is a disease that often causes difficulties in the maintenance of a normal level of blood glucose in a patient, mainly because either insufficient insulin is produced by the beta cells in the pancreas, or the body is unable to effectively utilise that insulin (Vaddiraju et al., 2010). The American Diabetes Association recommends a fasting plasma glucose level of 70–130 mg dl^{-1} for a normal person. If the glucose level is between 60–68 mg dl^{-1}, then the condition is called hypoglycaemia. If the glucose level is above 240 mg dl^{-1}, it is called hyperglycaemia. Both types of diabetes are a result of the dysregulation of the glucose level in the human body. A minimally invasive glucose sensor helps to monitor the glucose level and helps in the early diagnostic phase for the patients.

Currently, there are many invasive techniques used for the detection of glucose levels in the serum as well as various devices designed based on sensing techniques such as electroimpedance spectroscopy, enzyme oxidation, time domain reflectometer, and surface plasma resonance, potentiometic, voltammetric and amperometric techniques (Liu et al., 2013; Yonemori et al., 2009; Yan et al., 2011; Chou et al., 2013; Mahdi et al., 2012). Among these techniques, enzyme oxidation methods are the most reliable; however, these methods are invasive, have a serious disadvantage due to insufficient stability, and still require a technique for obtaining a blood sample (Vashist et al., 2011). It seems that a glucose sensor that does not require the use of enzymes, exhibits good stability, and can be reused is far from being practical because it requires the use of recent advanced fabrication processes (Kaimori et al., 2006).

The radio frequency (RF) detection method is one of the prospective candidates for the basis of a glucose sensor out of several detection methods available (Lee et al., 2011). RF technology can be applied to measure the characteristics of glucose by either a direct or combination method. The RF sensing technique is a good candidate for various types of biosensing applications such as DNA hybridisation, binding of biotin and streptavidin, and metamaterial and microwave glucose sensing (Lee et al., 2010; Spada et al., 2011). In this work, a label-free minimally invasive rectangular meandered line (RML) resonator functioning at a microwave frequency of 9.20 GHz was analysed for the detection of the glucose level in human serum and compared with an aqueous solution of deionised (D) water glucose solution (Kim et al., 2008). Glucose at

* Corresponding author.
E-mail addresses: nykim@kw.ac.kr (N.Y. Kim), aperioraj@gmail.com (R. Dhakal).

http://dx.doi.org/10.1016/j.bios.2014.10.021

different concentrations as a test analyte has different dielectric constants because the electrical properties depend upon the concentration. The detection of the glucose levels is based on the variation of the dielectric property with the different concentrations of glucose present in the serum and the change in the electrical behaviour due to the skin effect of the meandered conductive line (Abdalla et al., 2010). To increase the sensitivity of the resonator, an air-bridge structure is fabricated by using integrated passive device (IPD) technology on the top metal layer, which improves the sensitivity by increasing the magnitude of the return loss (S_{21}) by selective variation of bridge capacitance.

When an analyte is dropped onto the RF biosensor, changes will occur due to inductive and capacitive effects, which produce return losses and considerable shifts in the resonance frequency of the device. In the air-bridge area of the biosensor, the capacitance is proportional to the dielectric constant and the distance between the lower and upper conductive surfaces. The analyte then causes the change in the electrical behaviour of the biosensor mainly due to the capacitive effect.

2. Materials and methods

The first random sample of serum was selected with a glucose concentration ranging from 148 mg dl^{-1} to 268 mg dl^{-1} (sample 1), and a second random sample of serum was selected with a glucose concentration ranging from 105 mg dl^{-1} to 225 mg dl^{-1} (sample 2) (Peng et al., 2013). The sample was prepared by centrifugation at 3000 rpm for 12 min in the laboratory (Department of Biochemistry and Molecular biology, Medical College, Kyung Hee University, Seoul, S. Korea), separating whole blood into red blood cells (on the bottom) and serum (on the top of the test tube). Thus, the glucose concentration in the obtained serum was varied at a 20 mg dl^{-1} interval for seven different samples. At the same time, we also prepared an aqueous D-glucose solution with concentrations ranging from 25 mg dl^{-1} to 500 mg dl^{-1}. The data obtained from the D-glucose solution were then compared with the data obtained from the serum to determine relative shift in the resonance frequency.

2.1. Analytical process

The first step in the analytical development of a microwave resonator as a minimally invasive biosensor was performed using the electromagnetic simulation SONNET as shown in Fig. 1A. A sampled model of glucose (Fig. 1B) at different concentrations (from 25 mg dl^{-1} to 500 mg dl^{-1}) with a volume of 1-μl was implemented, which can create a reasonable shift in the resonance frequency for different concentrations. Next, for comparative analysis between the D-glucose and serum glucose levels, the process was again performed for two different samples of serum, with concentrations ranging from 148–268 mg dl^{-1} and 105–225 mg dl^{-1}, respectively. The experimental results for the transmission parameter (S_{21}) were obtained using an Agilent 8510C vector network analyser (VNA), and other decomposition parameters from the measurements were generated for further verification. The top surface of the chip was coated with Au to avoid unnecessary reaction, and the surface roughness was improved via an etching process to avoid the unnecessary loss of signal due to the skin effect, which improved the transmission parameter by minimising the signal loss.

The best surface morphological structures were generated after the physical plasma etching process with a root mean square (RMS) value of 63.66 nm. The parameters used for etching are as follows: an RF generator power of 150 W, an inductive coupled plasma (ICP) power of 1000 W, a total gas pressure of 7.5 mTorr, and a chamber temperature of 293 K. The resonator had total dimensions of 2 mm by 1.16 mm with a mounted air-bridge structure, used to provide increased sensitivity by improving the capacitive effect, on the surface of the chip. The input transmission line starts at the input ports, develops its meandered line structure, and ends on the opposite side. The device behaviour can be understood as a resonator for which the transmission parameters are affected by a top layer of different materials with a different dielectric constants; such a device ultimately helps in diagnosing the level of glucose in diabetes patients through the analysis of the serum.

2.2. Device concept and fabrication

The fabrication of the device started with the silicon nitride (SiN_x, 200 nm) passivation layer, which was first deposited over a gallium arsenide (GaAs, 400 μm) substrate using plasma enhanced chemical vapour deposition (PECVD). Next, a 2 μm-thick Au metal layer was formed by electroplating, which was used to form the metal lines for the meandered line structure of the resonator. Subsequently, a 20/80 nm Ti/Au seed metal was deposited by a RF sputtering process. The passivation layer is necessary to attain an even surface over any defects or roughness on the substrate surface. The passivation layer enhances the adhesion between the substrate and the first metal layer. Again, a seed metal layer was formed as previously described, followed by a second passivation layer of 200-nm SiN_x deposited via PECVD to prevent a possible electrical shortage between the first and second metal layers. Next, an air-bridge photo-process was performed prior to the Au (3 μm) air-bridge metal definition and plating process, by which the air-bridge interconnections were formed at broken coil paths around the metal beeline for the resonator, as shown in Fig. 1C. After the electroplating process, the air-bridge mask was stripped, and reactive ion etching of the Ti/Au seed metal was performed. The final fabricated device with an air-bridge structure is shown in Fig. 1C (Wang et al., 2011, 2010).

To analyse the application of the biosensor to real world situations, it was exposed to human serum from two different subjects with different concentration of glucose. The concentrations ranged from 148 to 268 mg dl^{-1} for the first sample and from 105–225 mg dl^{-1} for the second sample. The equivalent circuit modelling the entire process is shown in Fig. 1D, which consists of a parallel *LC* circuit, where L, C_g, and C_a represent the inductance of the meandered line, the capacitive component between the ground and the signal line, and the bridge capacitance formed by the glucose solution or the serum, respectively, as illustrated in Fig. 1E. The resonance frequency is described by

$$f = 1/2\Pi\sqrt{LC_a} \quad (1)$$

where the bridge capacitance (C_a) depends on the concentration of glucose because of the dependence of the dielectric constant on the glucose concentration. The C_a shown in Fig. 1D has a different value for the different solutions and ultimately generates the different resonance frequencies of the sensor characterised by Eq. (1) (Ahmadi and Jullien, 2009). The change in the electrical behaviour was caused by the concentration of electrons (e^-) on the outer surface of the resonator due to the inductive force, as illustrated in Fig. 1A. The RF biosensor was operating at a high operating frequency at an X-band of 9.20 GHz. Therefore, the electrons (e^-) are concentrated on the outer surface of the meandered conductive line and effectively generate a return loss and insertion loss that varies with the use of various glucose levels in serum, even for a minimum level of glucose.

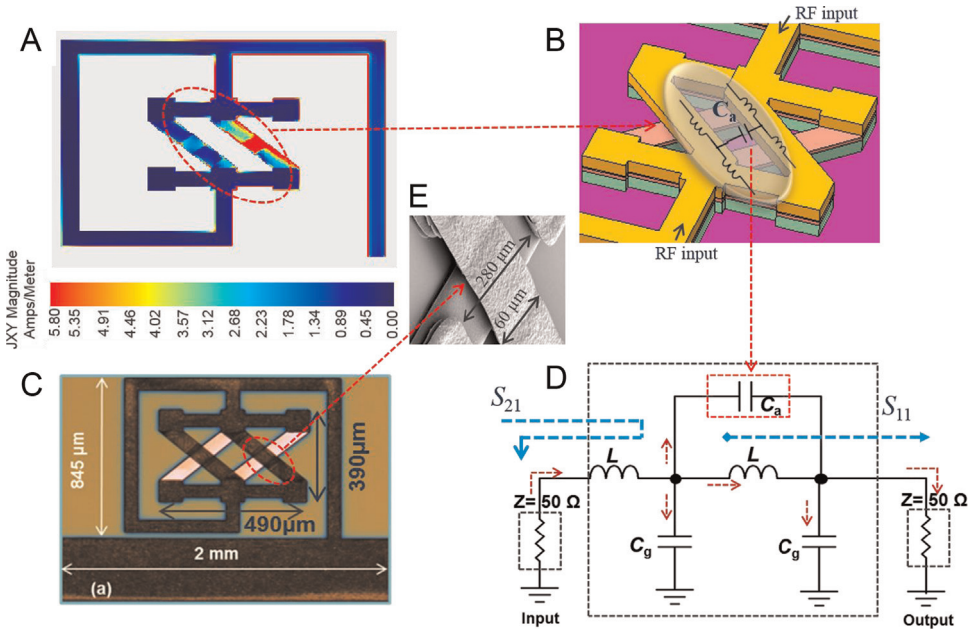

Fig. 1. Conception of serum glucose level detection using an RF resonator as a biosensor. (A) The current density showing the flow of current at the outer surface of the air-bridge structure measured at 9.20 GHz using the EM Simulator SONNET. (B) The sensitive part of the air bridge structure with bridge capacitance (C_a). (C) Fabrication of the biosensor with the IPD process. (D) The equivalent circuit model involving R, L, and C of the ports, after the serum was dropped on the biosensor. (E) The air-bridge structure by IPD.

2.3. RF detection and test

The RF detection of the glucose level is based on the resonance concept of the resonator. The biosensor produced a reasonable shift in the resonance frequency as well as a variation in the amplitude of the signal. The principle relies on the detection of the change in the RF signal caused by the volume of the analyte, which determines the dielectric parameters of a glucose molecule on the surface of the biosensor and is shown in Fig. 1D (Park et al., 2014; Liao et al., 2003). As a result, the biosensor can accurately demonstrate the minimum value of the resonance shift for different samples of the serum and the D-glucose solutions. The change in the S_{21} parameter and resonance shift was found to be due to the electromagnetic interaction between the biosensor and the glucose with a different dielectric constant (Kuranov et al., 2007; Venkatesh and Raghavan, 2004). Measurements of S_{21} and the fractional change in the resonance frequency of the resonator were monitored. We performed the experiment with 1-μl of D-glucose at a starting concentration of 25 mg dl^{-1} to analyse the resonance condition and to determine the resonance frequency. The process was further implemented with different concentrations of D-glucose up to 500 mg dl^{-1}. When the bare chip was exposed to D-glucose at different concentrations, due to the capacitive and inductive effects between the meandered-lines, the first resonance

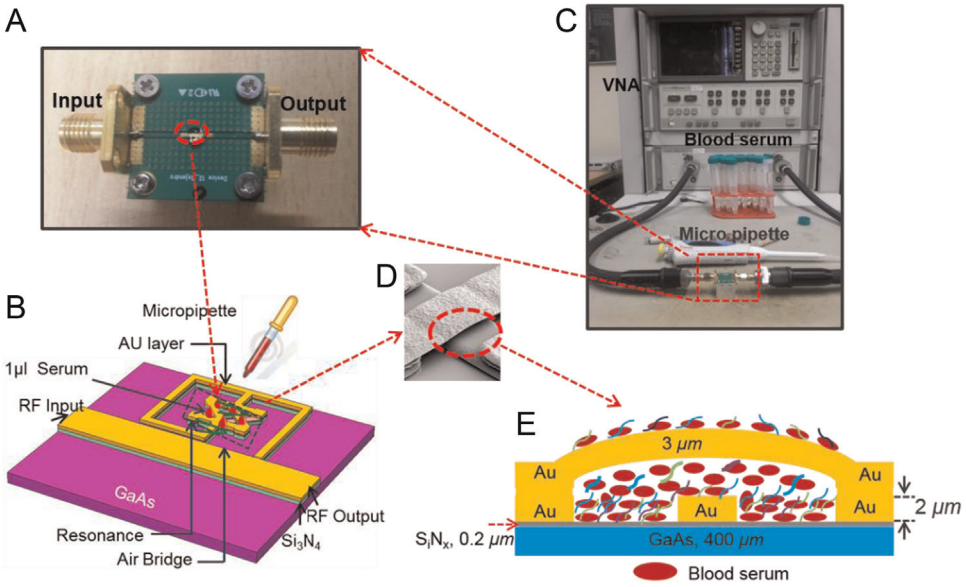

Fig. 2. Schematic diagram of (A) the final fabricated device packed in a printed circuit board (PCB) with a 50 Ω port connected on the input and output side to the transmission line for measurement. (B) The measurement concept, after the use of serum as a test analyte. (C) The experimental setup for biosensor measurement of the glucose level with the VNA. (D) Cross-section of the air-bridge structure. (E) Serum as an analyte was dropped on the surface of the biosensor covering the Au surface of 490 × 390 μm^2 consisting of an air-bridge structure.

condition for the minimum concentration of 25 mg dl^{-1} could be observed, as illustrated in Fig. 2A. The process was then executed with other concentrations of D-glucose to determine their respective resonance conditions.

After the first measurement with D-glucose, the structure was rinsed with a phosphate buffered saline solution (PBS) at pH=7 and deionised water. The nitrogen drying process was used before the next sample containing a different glucose concentration was analysed. Next, a 1-μl volume of serum of different glucose concentration were dropped by micro-pipette onto the surface of the resonator within the 490 μm by 390 μm area, as shown in Fig. 2B. The meandered-line structure contains a sensitive air-bridge structure with Au on the top surface, which generates a capacitive effect between the serum on the surface and above and below the air-bridge. Serum containing a different glucose concentration corresponds to a different dielectric property. This change in dielectric properties caused a shift in the resonance frequency from its initial resonance frequency.

For the final testing of the RML based biosensor, the sensor was packed in a PCB with a 50 Ω port connected on the input and output sides to the transmission-line. The ports were then connected to the two ports VNA, as shown in Fig. 2C. Before the final test with human serum and D-glucose, the RF measurement for the S_{21} characteristic of the resonator was obtained and called the bare resonance frequency. Next, 1-μl of serum containing glucose from the micro-pipette was dropped onto the air-bridge structure of the resonator chip, as illustrated in Fig. 2D and E. The best frequency response of the resonator was obtained by measuring the S_{21} and the correlation between the shifts in the resonance frequency (Tura et al., 2010). Subsequently, the device was again rinsed with PBS, at pH=7 and deionised water at an ambient temperature (25 °C) to ensure the stability of the device. The S_{21} parameter for the bare chip was again measured with no frequency shift, indicating that the signal was generated by the specific concentration of glucose in the serum. The measured bare resonance frequency after the test was found to exactly match the initial bare resonance frequency of 9.20 GHz. This result confirmed that the proposed device can be reused many times after the initial use by rinsing with PBS, which ensures the stability of the system.

To improve the conductivity on the resonator surface, we produced a pattern with the best surface morphological structure. Argon (Ar) plasma was used to adjust the surface roughness via etching, as shown in Fig. 3A. The top surface of the resonator plated with Au can be effectively etched by the Ar plasma for the generation of good surface morphological structure. Atomic force microscopy (AFM) images of the surface morphology were obtained, which determined that an RMS value of 63.66 nm was produced for 5 min of etching time. This alteration of the surface roughness with plasma etching treatment was performed to change the surface from a hydrophobic to a hydrophilic surface to increase the immobilisation rate of the glucose molecules and the resonance process.

3. Result and discussion

An RML resonator based biosensor for the biological detection of glucose levels in diabetes patients was demonstrated. The reusability

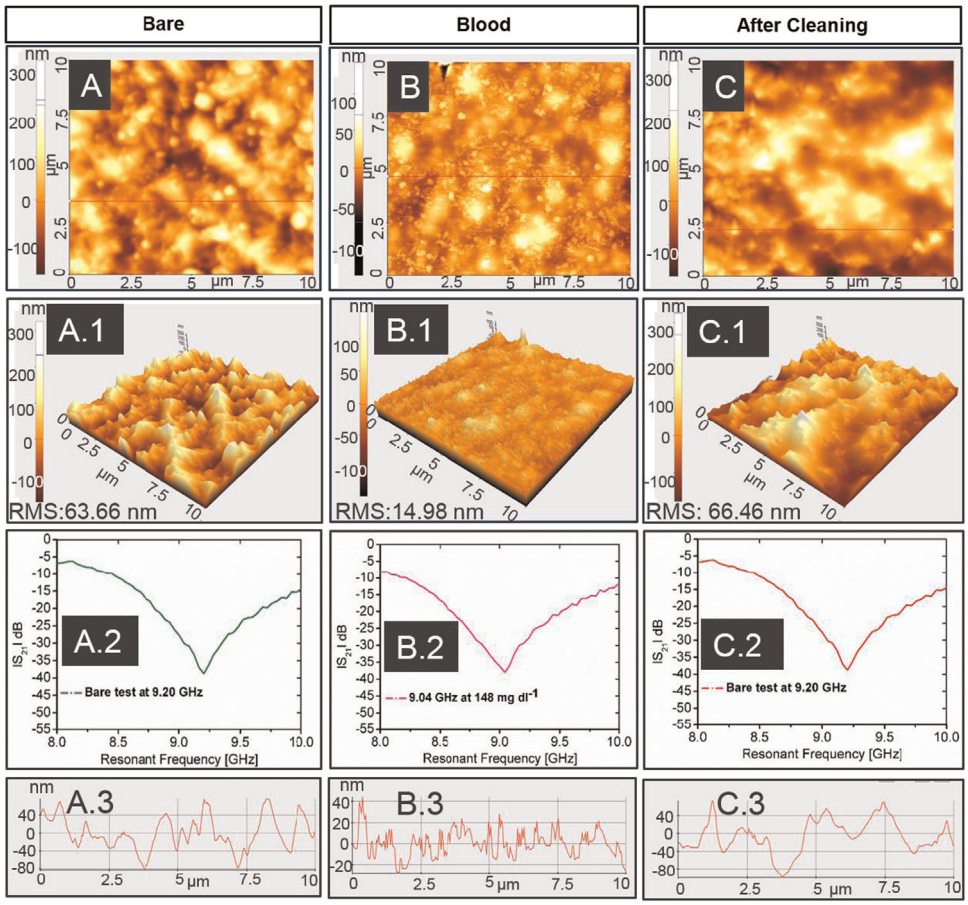

Fig. 3. Morphological analysis. (A) The 2-D view of the bare biosensor, 3-D surface profile (A.1), RF measurement of the device (A.2) and line profile graph for surface roughness (A.3). (B) The 2-D view of the biosensor with serum concentration of 148 mg dl^{-1}, 3-D surface profile (B.1), RF measurement (B.2) and line profile graph for the surface roughness (B.3) and (C) The 2-D view of the biosensor after test and washed with PBS, 3-D surface profile (C.1), RF measurement (C.2) and line profile graph for surface roughness (C.3).

of the proposed biosensor was verified by the resonance characteristics and further supported by morphological analysis of a bare chip, a chip with blood serum, and finally with a chip washed with PBS. Basically, two featured frequencies were observed: (a) a bare chip resonating at 9.20 GHz and (b) a chip after D-glucose or serum from the diabetes patients with different concentrations was dropped. From the two featured frequencies studied, we determine that we can obtain a reasonable shift in the resonance frequency for different glucose concentrations in the serum and D-glucose.

3.1. Reusability and surface characterisation

The reusability of the biosensor was characterised by measuring the resonance frequency before and after the use of serum and the D-glucose solution. We performed three different sets of experiments for each concentration of serum and D-glucose solution to observe the resonance frequency for each-iteration loop of the experiment. A total of 21 different experiments for each sample of the serum were tested and represented by the scatter plot, as shown in Fig. S1 (Supplementary section). No device response deterioration was observed over this long iteration of the measurement process. As a result, the relative standard deviation (RSD) of less than 1% was observed for each concentration of serum samples and aqueous solution of D-glucose. The observed data show no overlapping of the resonance frequency among the concentrations for different sets of the experiment. This observation validates that the proposed device can be reused many times after the initial use by rinsing with PBS. The bare resonance frequency from each set of experiments after rinsing was obtained at 9.20 GHz, which confirms the stability and reusability of the system.

To further assist the reusability of the biosensor, an intensive study with morphological analysis of the top sensing surface at a concentration of 148 mg dl^{-1} was performed for three consecutive iterations for a single device (Xu et al., 2009). We produced a pattern, with the best surface morphological structure with an RMS value of 63.66 nm at 5 min etching time. The standard deviation (SD) for the bare biosensor, the biosensor with human serum, and the biosensor after cleaning was found to be 1.20, 1.92, and 1.22, respectively. This result signifies that the RMS values for each experiment are very much correlated. Table S1 (Supplementary section) indicates the clear variation of the RMS value for different stages of the experiment. The value with the lowest RMS was selected for further analysis. The 2-D and 3-D view of a bare biosensor with an RMS value of 63.66 nm and resonance frequency of 9.20 GHz are shown in Fig. 3A, A.1 and A.2. Next, the chip exposed to human serum with the concentration of 148 mg dl^{-1} resulted in a RMS value of 14.98 nm (Fig. 3B and B.1) with a resonance frequency of 9.04 GHz (Fig 3B.2). From Fig. 3B, it is clear that the deposition of blood particles creates uneven peaks and valleys of the surface, resulting in a relatively even distribution on the surface with a minimum RMS value compared to the bare device, as indicated by line profile for the surface morphology (Fig 3B.3). Next, the device was rinsed with PBS and dried by nitrogen gas. After the testing of the device, the obtained RMS value of 66.46 nm (Fig. 3C and C.1) and resonance frequency of 9.20 GHz (Fig. 3C.2) ensured the reusability of the device for the future use. The surface roughness profiles, before (Fig. 3A.3) and after (Fig. 3C.3) the test were concluded to be similar. The process further verified that there is no chemical immobilisation involved, which can alter the resonance frequency from returning to its initial position (Park et al., 2006).

3.2. RF response of the device

The transmission parameters clearly reflect the electrical behaviour of the device (Moore, 2009; Park et al., 2012). In this study, we measured the transmission parameter of a device for two different types of subjects: human serum and D-glucose, as illustrated in Fig. 4. The biosensor with the bare Au surface exhibiting the resonance at 9.20 GHz is called the bare resonance frequency. For all of the patterns, the resonance peak shifts downward with decreasing amplitude with an increase in the glucose concentration. The resonance frequency of the D-glucose solution varied in the range from 8.68 to 9.12 GHz with a

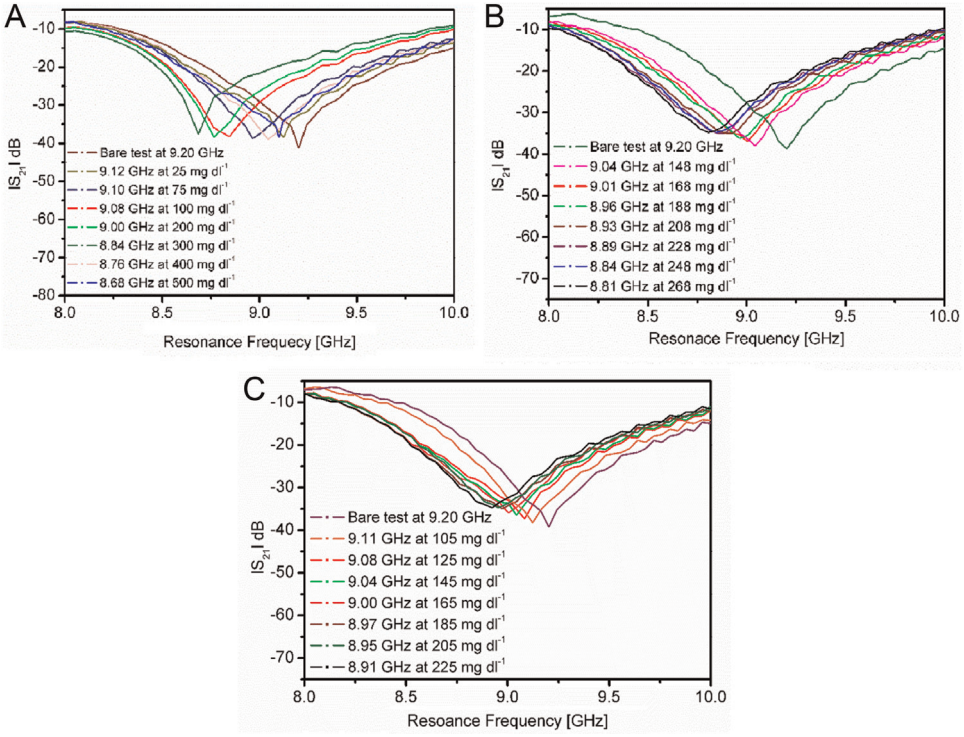

Fig. 4. Variation in the resonance frequency with amplitude variation. (A) Aqueous D-glucose solution. (B) Human serum (sample 1) with base a glucose concentration of 148 mg dl^{-1} and (C) Human serum (sample 2) with a base glucose concentration of 105 mg dl^{-1}.

tolerable shift in resonance frequency as shown in Fig. 4A. The sensor generated a maximum shift of 160 MHz and 90 MHz for the minimum glucose levels of 148 mg dl^{-1} and 105 mg dl^{-1} for serum samples 1 and 2 (Fig. 4B and C), respectively. The device exhibited good sensitivity in detecting 1.08 MHz and 0.85 MHz changes for the corresponding 1 mg dl^{-1} changes in the glucose concentrations in serum samples 1 and 2, respectively.

3.3. Effect of the measurement time

The sensitivity of the device is reflected by the time required for the final output. To analyse the effectiveness of the proposed biosensor, we measured the response to D-glucose at different time intervals, namely, one, two, three and four minutes, and obtained a regression plot for the shift in resonance frequency, as shown in Fig. S2 (Supplementary section). The time varying calibration curve is generated by dropping 1-μl of D-glucose with a concentration ranging from 25–500 mg dl^{-1} for different time (t) intervals of up to four min at an interval of one minute. The device exhibits a minimum shift of 0 MHz and maximum shift of 80 MHz for the measurement time interval of four minutes and one minute, respectively, at a minimum concentration of 25 mg dl^{-1}. The rapid response and excellent results with a tolerable shift in the resonance frequency are obtained for the measurement time interval of 60 s at a minimum glucose concentration of 25 mg dl^{-1}, which demonstrates the enhanced real-time identification of the glucose level.

3.4. Calibration curves for the analysis of serum and D-glucose

We investigated the effect of an aqueous solution of D-glucose and blood serum on the resonance frequency of the device. To obtain the optimised performance of the device, we conducted experiments with different samples of serum as well as a D-glucose solution with different glucose concentrations. Three different measurements for the two different serum samples and D-glucose solution were conducted. Eq. (2) represents the regression line for the D-glucose solution with the minimum shift of 80 MHz from the initial bare resonance frequency, as represented in Fig. S3 (Supplementary section).

The calibration curve represented by Eqs. (3) and (4) were generated from two different human serum samples by dropping 1-μl of serum with glucose concentrations in the range of 148–268 mg dl^{-1} and 105–225 mg dl^{-1} (Fig. 5A and B), respectively. The regression value of 0.9973 generated for serum sample 1 is higher than the regression value of 0.9928 generated for serum sample 2. This small inconsistency in the regression value (R^2) for the serum sample was caused by the uncertainties in the preparation of seven different glucose concentration levels achieved from the standard addition technique. Each concentration level was prepared from the real sample of blood having unique base glucose concentration level. Identical environment and criteria cannot be realised practically for both the real samples, so that there was slightly variation in the relative frequency shift and so to the correlation coefficient. Both the samples were prepared in the laboratory by the biological process in which each samples were treated separately to prepare different concentration levels of glucose.

The analysis indicated that the resonance approach of identifying the glucose level can be applied to the serum for detection of the glucose level. Table 1 summarises the resonance frequency variation with different concentrations of D-glucose and blood serum. We obtained a minimum shift of 80 MHz in the resonance frequency for a minimum D-glucose concentration of 25 mg dl^{-1}. A minimum shift of 0.4 MHz corresponding to a 1 mg dl^{-1} change in the glucose level was also obtained. The sensing limitation of our device, known as the limit of detection (LOD) was calculated as 8.01 mg dl^{-1} and 13.20 mg dl^{-1} for serum samples 1 and 2, respectively. In addition, the limit of quantisation (LOQ) was estimated to be 24.30 mg dl^{-1} and

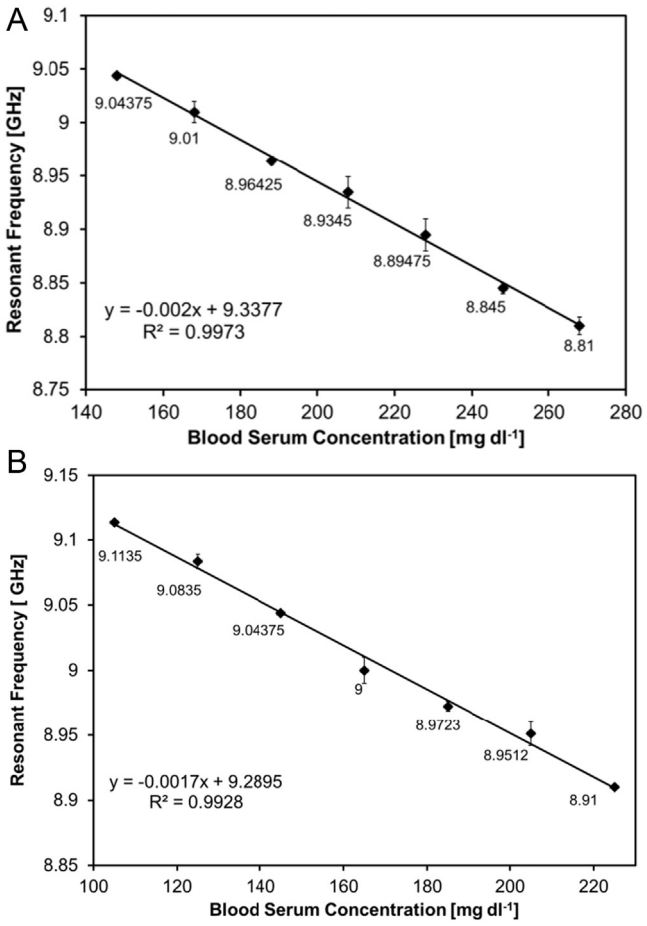

Fig. 5. Regression analysis for the shift in the resonance frequency with the error bars for (A) human serum (sample 1) with a base glucose concentration of 148 mg dl^{-1} and (B) human serum (sample 2) with a base glucose concentration of 105 mg dl^{-1}. The error bars indicate deviation of resonance peak for n=7 (RSD < 1%).

40 mg dl^{-1} for serum samples 1 and 2, respectively. The nature of the calibration curves and the data obtained from the frequency shifts with an RSD of less than 1% for each sample of serum indicates a small spread of the resonance frequencies for a particular concentration. These results are outstanding compared to the results of other methods having a response time of 15 min and values for the LOD of 25 mg dl^{-1} (Mamdouh et al., 2014), 12.02 mg dl^{-1} (Kim et al., 2013) and 36.6 mg dl^{-1} (Ruifen et al., 2012), suggesting that this approach can be applied to distinguish the level of glucose in diabetes patients. The comparative analysis based on the performance is summarised in Table S2 (Supplementary section). The calibration curves for D-glucose and human serum can be fitted by the following equations:

$$Y_1[\mathrm{GHz}] = -0.001 \times X[\mathrm{mg\ dl^{-1}}] + 9.1673, \quad \text{for aqueous solution of } D\text{–glucose Regression}\left[R^2\right] = 0.9857 \tag{2}$$

$$Y_2[\mathrm{GHz}] = -0.002 \times X[\mathrm{mg\ dl^{-1}}] + 9.3377, \quad \text{for serum (sample 1) Regression}\left[R^2\right] = 0.9973 \tag{3}$$

Table 1
Comparison of the glucose levels in a standard solution of D-glucose and in two different serum samples.

[a]S.N	D-glucose			Human serum					
	Concentration (mg dl^{-1})	[b]f_1 (GHz)	[c]RSD (%)	Sample 1 concentration (mg dl^{-1})	[b]f_2 (GHz)	[c]RSD (%)	Sample 2 concentration (mg dl^{-1})	[b]f_3 (GHz)	[c]RSD(%)
1	500	8.68	± 0.23	268	8.81	± 0.11	225	8.91	± 0.11
2	400	8.76	± 0.17	248	8.84	± 0.24	205	8.95	± 0.17
3	300	8.84	± 0.23	228	8.89	± 0.17	185	8.97	± 0.11
4	200	9.00	± 0.86	208	8.93	± 0.17	165	9.00	± 0.11
5	100	9.08	± 0.17	188	8.96	± 0.11	145	9.04	± 0.11
6	75	9.10	± 0.10	168	9.01	± 0.22	125	9.08	± 0.17
7	25	9.12	± 0.11	148	9.04	± 0.17	105	9.11	± 0.17
8	Bare test	9.20	0	Bare test	9.20	0	Bare test	9.20	0

[a] S.N denotes the serial number.
[b] f_1, f_2 and f_3 denotes the resonance frequencies for the different cases.
[c] RSD denotes the relative standard deviation.

$$Y_3[\mathrm{GHz}] = -0.0017 \times X\ [\mathrm{mg\ dl^{-1}}] + 9.2895, \quad \text{for serum (sample 2)Regression}\left[R^2\right] = 0.9928 \tag{4}$$

4. Conclusion

A reusable robust RF biosensor with an IPD air-bridge type resonator was fabricated on a GaAs substrate for testing the glucose level in serum samples with base glucose concentrations of 148 mg dl^{-1} and 105 mg dl^{-1}. The serum (sample 1) with a glucose concentration of 148 mg dl^{-1} generated an LOD of 8.01 mg dl^{-1} and an LOQ of 24.30 mg dl^{-1} and the serum (sample 2) with a glucose concentration of 105 mg dl^{-1} generated an LOD of 13.20 mg dl^{-1} and an LOQ of 40 mg dl^{-1}. The studied biosensor provided a rapid response for each of the serum samples within the linear calibration ranges of 148–268 mg dl^{-1} and 105–225 mg dl^{-1}, with correlation coefficients of 0.9973 and 0.9928, respectively. This finding indicated the development of resonance-based sensing with the excellent sensitivity of 1.08 MHz and 0.85 MHz per 1 mg dl^{-1} for samples 1 and 2, respectively. For a glucose level between 25–500 mg dl^{-1}, the biosensor exhibited outstanding characteristics with an observed shift of 80 MHz for a minimum concentration of 25 mg dl^{-1}, which is a clear indication of the glucose level detection. Moreover, the morphological analysis of this RF biosensor validates the robust reusability for the real time detection of the glucose level in the whole blood of diabetes patients during the point of care testing.

Acknowledgements

This research was supported by Basic Science Research Program through the National Research Foundation of Korea (NRF) funded by the Ministry of Science, ICT & Future Planning (No. 2011-0030079) and a grant supported from the Korean government (MEST) No. 2012R1A1A2004366. This work was also supported by a Research Grant of Kwangwoon University in 2013. Authors acknowledge to Professor Sung-Soo Kim and Research Professor Jo Young Hwa, Department of Biochemistry and Molecular Biology, Medical College, Kyung-Hee University, Seoul, S. Korea. Additionally, we thank Mr. Ho-Kun Sung from the Korean Advanced Nano Fab Centre (KANC) for his technical support with the materials and circuit fabrications during this work.

Appendix A. Supplementary material

Supplementary data associated with this article can be found in the online version at http://dx.doi.org/10.1016/j.bios.2014.10.021.

References

Abdalla, S., Al-ameer, S.S., Al-Magaishi, S.H., 2010. Biomicrofluidics 4, 034101.
Ahmadi, M.M., Jullien, G.A., 2009. IEEE Trans. Biomed. Circuits Syst. 3, 169–180.
Chou, J.C., Cheng, T.Y., Ye, G.C., Liao, Y.H., Yang, S.Y., Chou, H.T., 2013. IEEE. Sens. J. 13, 4180–4187.
Kaimori, S., Kitamura, T., Ichino, M., Hosoya, T., Kurusu, F., Ishikawa, T., Nakamura, H., Gotoh, M., Karube, I., 2006. Anal. Chim. Acta 573–574, 104–109.
Kim, D.M., Kim, M.Y., Reddy, S.S., Cho, J., Cho, C.H., Jung, S., Shim, Y.B., 2013. Anal. Chem. 85, 11643–11649.
Kim, J.C., Babajanyan, A., Hovsepyan, A., Lee, K.J., Friedman, B., 2008. Rev. Sci. Instrum. 79, 086107.
Kuranov, R.V., Sapozhnikova, V.V., Prough, D.S., Cicenaite, I., Esenaliev, R.O., 2007. J. Diabetes Sci. Technol. 1, 470–477.
Lee, H.J., Lee, H.S., Yoo, K.H., 2010. J. Appl. Phys. 108, 014908.
Lee, H.J., Lee, J.H., Jung, H.I., 2011. Appl. Phys. Lett. 99, 163703.
Liao, X.J., Raghavan, G.S.V., Dai, J.M., Yaylayan, V.A., 2003. Food Res. Int. 36, 485–490.
Liu, M.M., Liu, R., Chen, W., 2013. Biosens. Bioelectron. 45, 206–212.
Mahdi, J.F., Helambe, S.N., Akhter, N., 2012. J. Chem. Biol. Sci. B 2, 1431–1437.
Mamdouh, A., Joshua, T., Jessica, P., Ramella, C., Kim, S., R., 2014. Sensors 14, 12127–121448.
Moore, B., 2009. J. Diabetes Sci. Technol. 3, 180–183.
Park, H.G., Yoon, S.H., Patil, U., Anoop, R., Lee, J.H., Lim, J.H., Lee, W.H., Jun, S.C., 2014. Biosens. Bioelectron. 54, 141–145.
Park, S.J., Boo, H.K., Chung, T.D., 2006. Anal. Chim. Acta 556, 46–57.
Park, S.Y., Park, S.J., Jeong, R.A., Boo, H.K., Park, J.Y., Kim, H.C., Chung, T.D., 2012. Biosens. Bioelectron. 31, 284–291.
Peng, B., Lu, J., Balijepalli, A.S., Major, T.C., Cohan, B.E., Meyerhoff, M.E., 2013. Biosens. Bioelectron. 49, 204–209.
Ruifen, H., Adrian, C.S., Christopher, R.L., 2012. Biosens. Bioelectron. 35, 425–428.
Spada, L.L., Bilotti, F., Vegni, L., 2011. Prog. Electromagn. Res. B 34, 205–223.
Tura, A., Sbrignadello, S., Cianciavicchia, D., Pacini, G., Ravazzani, P., 2010. Sensors 10, 5346–5358.
Vaddiraju, S., Burgess, D.J., Tomazos, I., Jain, F.C., Papadimitrakopoulos, F., 2010. J. Diabetes Sci. Technol. 4, 1540–1562.
Vashist, S.K., Zheng, D., Al-Rubeaan, K., Luong, J.H.T., Sheu, F.S., 2011. Anal. Chim. Acta 703, 124–136.
Venkatesh, M.S., Raghavan, G.S.V., 2004. Biosyst. Eng. 88, 1–18.
Wang, C., Lee, J.H., Kim, N.Y., 2010. Microw. Opt. Technol. Lett. 52, 618–623.
Wang, C., Lee, W.S., Zhang, F., Kim, N.Y., 2011. Int. J. Adv. Manuf. Technol. 52, 1011–1018.
Xu, Q., Zhao, Y., Xu, J.Z., Zhu, J.J., 2009. Sens. Actuators B 114, 379–386.
Yan, Q.Y., Peng, B., Su, G., Cohan, B.E., Major, T.C., Meyerhoff, M.E., 2011. Anal. Chem. 83, 8341–8346.
Yonemori, Y., Takahashi, E., Ren, H.F., Hayashi, T., Endo, H., 2009. Anal. Chim. Acta 633, 90–96.